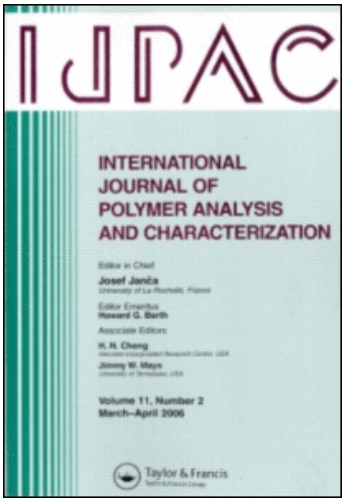

International Journal of Polymer Analysis and Characterization
Publication details, including instructions for authors and subscription information:
http://www.informaworld.com/smpp/title~content=t713646643

Conductive Carbon Loaded Polymer Film Electrodes for Pulsed Power Applications. Part II: Determination and Minimization of the Contact Resistance

Bart Roodenburg[a]; P. G. Malchev[b]; Sjoerd W. H. de Haan[a]; Telma I. V. Leitão[b]; J. A. Ferreira[a]
[a] Delft University of Technology, EEMCS, Delft, The Netherlands [b] Delft University of Technology, TNW-Chem Tech, Delft, The Netherlands

To cite this Article Roodenburg, Bart , Malchev, P. G. , de Haan, Sjoerd W. H. , Leitão, Telma I. V. and Ferreira, J. A.(2009) 'Conductive Carbon Loaded Polymer Film Electrodes for Pulsed Power Applications. Part II: Determination and Minimization of the Contact Resistance', International Journal of Polymer Analysis and Characterization, 14: 1, 1 — 18
To link to this Article: DOI: 10.1080/10236660802553533
URL: http://dx.doi.org/10.1080/10236660802553533

International Journal of Polymer Anal. Charact., 14: 1–18, 2009

ISSN: 1023-666X print
DOI: 10.1080/10236660802553533

Taylor & Francis
Taylor & Francis Group

Conductive Carbon Loaded Polymer Film Electrodes for Pulsed Power Applications. Part II: Determination and Minimization of the Contact Resistance

Bart Roodenburg,[1] P. G. Malchev,[2] Sjoerd W. H. de Haan,[1] Telma I. V. Leitão,[2] and J. A. Ferreira[1]
[1]Delft University of Technology, EEMCS, Delft, The Netherlands
[2]Delft University of Technology, TNW-Chem Tech, Delft, The Netherlands

Abstract: Electrically conductive polymer composites consisting of a nonconductive polymer matrix and conductive fillers, such as carbon black, are widely used. This contribution describes a newly developed measurement setup that has been built to investigate the specific electrical properties of polymer composite films for pulsed conditions in the microsecond (10^{-6} s) range. For an industrially available volume conductive polymer film (Carbostat) the contact resistivity to copper has been investigated. Also, three methods for minimizing the contact resistivity, namely pressing, gluing, and wetting, have been compared for a wide range of applied current densities.

Keywords: Contact resistance; Plastic electrodes; Polymer composite; Pulsed power

Submitted 15 July 2008; accepted 17 September 2008.
This project is supported by the Dutch Technology Foundation STW, which is a division of the Dutch Organisation for Scientific Research NWO.
Correspondence: Bart Roodenburg, Delft University of Technology, EEMCS, Mekelweg 4, 2628CD Delft, The Netherlands. E-mail: B.Roodenburg@ewi.tudelft.nl

INTRODUCTION

Nonconductive thermoplastic polymer films are traditionally used as a packaging material for food as well as nonfood products. For some packaging applications, like for electronic components, a specific degree of electrical conductivity is required, for example, for electrostatic discharge (ESD) protection. Since polymers are usually electrical insulators with a typical conductivity of $\sim 10^{-12}$ S/m,[1] one method to increase the electrical conductivity of a polymer is by the addition of different conductive fillers, thus creating a conductive polymer composite.[2–8]

Unique mechanical and electrical properties, like the current limiting effect due to their positive temperature coefficient,[9,10] makes it possible to explore conductive polymers as electrodes in newly developed pulsed power applications. By applying short pulses, the current density can be increased before breakdown will occur, and this will expand the number of applications. Most industrially available polymer specifications are based on a certain application area (e.g., ESD protection, electromagnetic interference (EMI) shielding, or capacitor foils [9–12]). They do not describe the properties for pulsed applications. In the international standard for resistivity measurements on composite conductive plastics, only a method for DC has been specified,[13,14] where it is noted that the contact resistance can dominate the sample resistance. So resistivity parameters specified by manufacturers can be largely influenced by the contact resistance.

The results on film properties and the contact resistance measurements are described in two separate articles, part I[15] and this part II. To be able to adequately investigate the film properties for pulsed power applications, a setup is needed that can apply high voltage pulses to the polymer sample and reduces the effect of the contact resistance to a minimum. This newly developed measurement setup, which is described in this part II, has been used to characterize the industrially available film Carbostat. Part II also describes a systematic analysis of contact resistance between the characterized polymer film and a copper electrode, and three contact resistance minimization methods, pressing, wetting and gluing. The experiments shown have been carried out in the microsecond (10^{-6} s) pulse range and are compared with DC measurements.

Conductive Composite Polymers

Figure 1 shows the typical form of the conductivity dependence of a conductive composite material on the conductive filler content. Upon an increase of the filler concentration, a critical value, Φ_c, is reached above which the conductivity of the composite rapidly increases. Within the

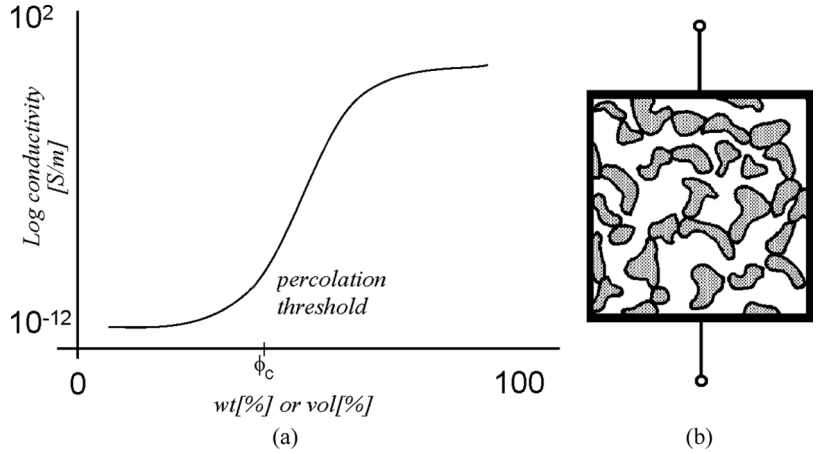

Figure 1. (a) Typical conductivity dependence of a conductive composite material on filler content, (b) schematic representation of the composite after percolation.[14]

percolation theory framework this concentration is referred to as percolation threshold.[16] Below this concentration, the filler particles are separately dispersed or form isolated clusters of finite size distributed within the polymer matrix. At Φ_c, however, the clusters become interconnected and produce an infinite continuous path of conductive particles within the insulating matrix, which allows a current to flow through the composite material.

Considered Material

The industrially available composite film Carbostat, which is used in this study, is based on ethylene vinyl acetate copolymer (EVA) and is filled with 30 wt% carbon black (CB).[17] The film has a typical thickness of 80 μm. During processing of films, the thermoplastic molecules gain some orientation, which makes the macroscopic properties of stretched polymers such as strength and optical and electrical properties depend on direction. The typical conductivity in normal (i.e., perpendicular) direction and parallel direction are in the range of 0.1–0.9 S/m and 5.0–7.9 S/m respectively. For the electrical characterization described in this contribution, two production batches of Carbostat film have been used, batches no. 08/2005 and 06/2006. Detailed information on the mechanical and electrical behavior of Carbostat can be found in part I[15] of this contribution.

CONTRIBUTORS TO RESISTANCE

A film sample that is connected between two electrodes is a series connection of two resistances, namely the contact resistance and film resistance. These resistances can be strongly influenced by temperature, pressure, and applied electric field. The following contributors that will influence the measured resistance have been investigated:

- Time- and pressure-dependent film conductivity, part I
- Electric field-dependent film conductivity, part I
- Contact resistance, part II

The measurements, which were described in part I, were carried out to determine the film characteristics without contact resistance. During these measurements, the contact resistance was eliminated by using conductive glue. Glued electrode connections are possible for fixed applications; for applications that have to be changed within a certain time frame, non-fixed solutions are needed. In this part the contact resistivity between bare electrodes and wetted electrodes has been investigated and compared with the resistivity of glued electrodes. The procedure to investigate the contact resistivity between polymer film and copper is depicted in Figure 2.

Applications that have to deal with interface problems between different materials are widespread, e.g., in circuit breaker contacts or

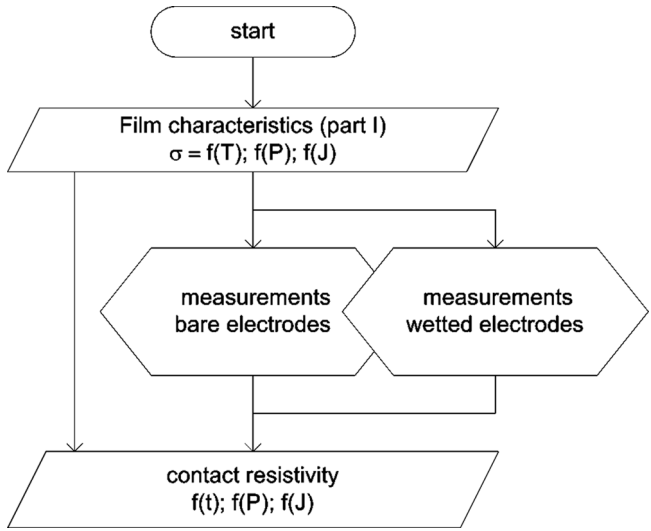

Figure 2. Process flowchart for the determination of the contact resistivity.

on potentiometer tracks.[18,19] There can be two reasons to reduce the contact resistance: good thermal conductivity can be needed[20] or high electrical conductivity. This contribution focuses on the latter. The main goal is to distribute the electrical current homogeneously across the interface to avoid local i^2R losses and thereby too early breakdown of the polymer.

Contact Resistance

Contact resistance is the resistance caused by a nonideal contact between two materials, which is shown in Figure 3. Generally determined as insulating areas between the two materials, it is caused by nonideal flat surfaces and insulating oxide layers. The total resistance or the measured resistance from material a to material b can be determined by the measured voltage (u_m) and current (i_m) and equals

$$R_m = \frac{u_m}{i_m} = \frac{l_a}{\sigma_a A} + R_c + \frac{l_b}{\sigma_b A} \tag{1}$$

where l is the length of the specified material in [m], σ is the conductivity of that material in [S/m], A is the cross-sectional area in [m^2], and R_c is

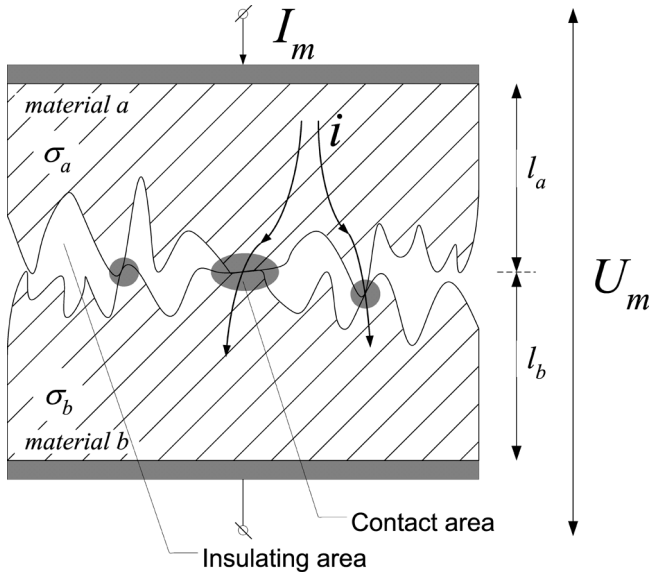

Figure 3. Detailed interface between two materials with a certain roughness; the grey parts represent areas where both materials make an electrical contact and the white represents the electrical insulating areas.

the contact resistance in [Ω]. In general the contact resistivity, r_s, or specific contact resistance in [$\Omega \cdot m^2$], which characterizes the resistance independent from the contact area, is defined as the slope of the current-density-voltage curve of the contact transition.[21] The contact resistivity equals

$$r_s = \left(\frac{\partial U_c}{\partial J_c}\right) = R''_m - \frac{l_a}{\sigma_a} - \frac{l_b}{\sigma_b} \tag{2}$$

where J equals the current density in [A/m^2] and R''_m is the measured resistance per unit area [$\Omega \cdot m^2$]. This form is the most frequently used in practical applications to determine r_s. One explicit value for r_s can be given only for contacts that are sufficiently ohmic within the range of current density under study. When n different materials are involved in the current conduction path the sum of the total contact resistivity equals

$$r_{s\_tot} = R''_m - \sum_n \frac{l_n}{\sigma_n} \tag{3}$$

For metal conductors, the conductivity, σ, generally does not depend on the voltage and hence not on the electric field. Polymer composites conductivity, on the contrary, does depend on the applied electric field, so $\sigma = f(E)$, and therefore the determination of the contact resistivity without consideration of the electric field is not applicable.

Reduction of contact resistance can be achieved, in general, by pressing or gluing both materials together or by contact wetting, which is commonly known for micro-relays.[22] Pressing and wetting both result in a larger contact area and thereby lower contact resistance. Softer materials like gold or tin tend to form larger contact areas.[23] Metal oxides, which are mainly nonconductive, are often present on the interface. Here also nonreactive materials, like gold or tin (-plated contacts) result in lower contact resistances because of the absence of oxides. In general, clean nonoxidized contacts result in lower contact resistance.

For electronic applications with conductive polymers, a joint between a metal (e.g., copper) and the conductive polymer film needs to be made.[24] Due to the surface roughness and low stiffness of the film it will creep (i.e., flow plastically) from high pressure areas (peaks in Figure 3) into the insulating areas, which results in a lower contact resistance between metal and film. This process has a typical time constant of 1–100 s. If the film is too thin to fill all noncontacting areas the reduction in contact resistance is not optimal. A too thick film, on the contrary, adds extra bulk resistance and thereby losses. Generally, a larger ratio between film thickness and average electrode roughness will result in lower contact resistivity. Also, the roughness of the polymer film, elasticity, and the filler

particle size have influence on the contact resistivity behavior. Both contact resistivity reduction methods, fixed by electrical glue and wetting, are described and tested in the next sections.

High Electric Fields

For applications especially in (pulsed) power equipment, the current density and the achieved field strength in the material will be high. The composite polymer film, filled with small CB grains, is loaded locally with even higher electric fields strengths, which results in a lower film resistance due to so-called hopping conduction[2] and finally in breakdown of the polymer.[25] Breakdown due to local high electric fields caused by sharp inclusions is generally known as treeing.[26] This can also happen at sharp particles or protrusions on the electrodes and is also able to initiate a breakdown at the interface, which also lowers the contact resistance locally.

MEASUREMENT SETUP

Characterization of the polymer film and its contact resistance is possible only when the copper wires, which are used for measurements, can be (re)connected to the sample with a great reproducibility. Otherwise one is not able to compare the different measurements with each other. To ensure the reproducibility of the measurements a mechanical clamp has been developed.

Clamped Samples

Figure 4 shows the clamp that was used to determine the electrical behavior of the film and the contact resistivity to the electrodes. It consists of four copper electrodes, which also make determination of surface resistivity, parallel volume resistivity, and perpendicular volume resistivity of the film possible.

The two top electrodes and two bottom electrodes that form the effective $1140\,\text{mm}^2$ electrode surface area are $19 \times 19 \times 90\,\text{mm}$ and $19 \times 19 \times 60\,\text{mm}$ respectively. Both top electrodes can slide along two metal studs and are equipped with a set of compression springs that realizes the needed contact force. The total force on the film sample and the electrode area results in the applied pressure (stress) on the film and equals

$$P_c = \frac{2c_s(s_0 - s_x) \pm m_t g}{A} \tag{4}$$

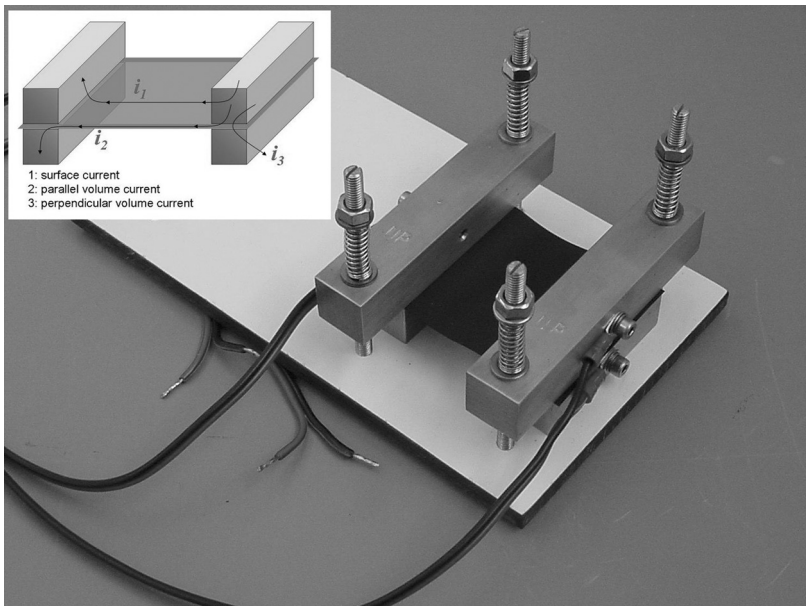

Figure 4. Typical construction of the clamp with spring assembly and four separate copper electrodes.

where P_c is the clamp pressure in [Pa], c_s is the spring constant in [N/mm], s_0 is the equilibrium length of the spring in [mm], s_x is the spring length in loaded condition in [mm], m_t is the mass of the top electrode in [kg], g is the gravity in [m/s^2], and A is the electrode area in [m^2]. Forces lower than $m_t g$ can be achieved by turning the clamp upside down. With this clamp, pressures up to 35 kPa can be applied. The contact surfaces are face milled and polished. For each experiment they were cleaned with a Scotch-Brite Grade 400 pad and degreased with alcohol. Examination of the surface roughness was done and resulted in an arithmetic average (i.e., so-called R_a value), which is the average of the absolute values on the vertical deviations of the roughness profile from the mean line, of 0.25 μm and 0.2 μm longitudinally and in cross direction of the electrode respectively. Roughness measurements were carried out with a Mitutoyo SJ-301 tester. The ratio between film thickness and R_a equals 320–400. The ratio between the CB filler particles and R_a equals 0.2–1, which is rather low. Particles located at the surface of the polymer film do not fit well in the roughness profile of the electrode, which results in less used contact area.

Wetted Samples

The above described clamp was also used for contact resistivity measurements in wetted conditions. The liquid, which is an aqueous solution, was kept in position with ribbon gauze as shown in Figure 5. This aqueous solution contains demineralized water ($\sigma_w < 1\,\mu S/cm$) added with 0.1 mol/L (i.e., 0.58 wt%) NaCl.[27] The obtained conductivity of this electrolytic interfacial liquid is approximately 1 S/m, which is near to the conductivity of the polymer film to obtain a homogeneously distributed electric field. Wetting will result in a better utilization of the contact area because it will fill the insulative areas as depicted in Figure 3. The main drawback is that the current conduction in an electrolyte takes place via ions instead of electrons. This can lead to irreversible electrode (*Red-ox*) reactions and that will change the chemical nature and the conductivity of the interfacial liquid. The preferred reactions are the reduction of water and the oxidation of chloride ions at cathode and anode respectively.[28]

Electronic Setup

Together with the clamp, to ensure the reproducibility of the measurements, a special electronics circuit has been developed that generates damped

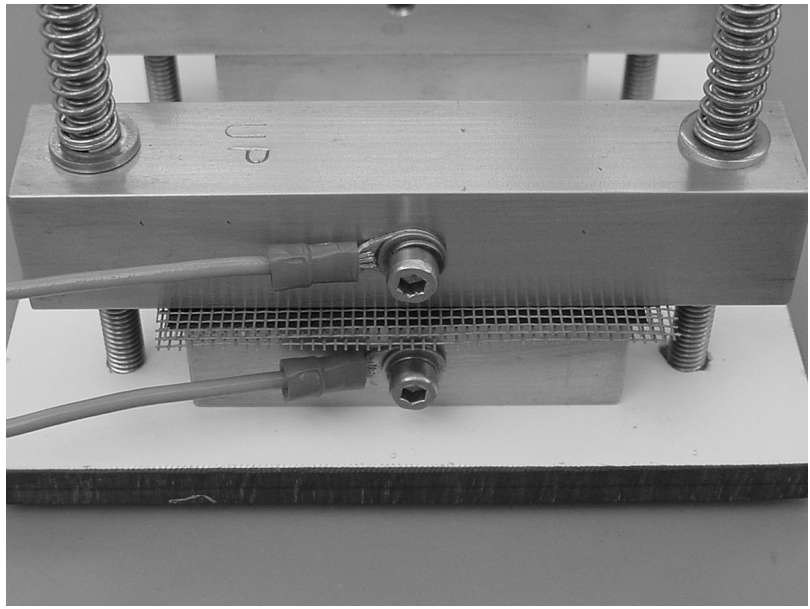

Figure 5. Wetted film sample between ribbon gauze. Material buildup: copper bar, water-filled gauze, film, water-filled gauze, and copper bar.

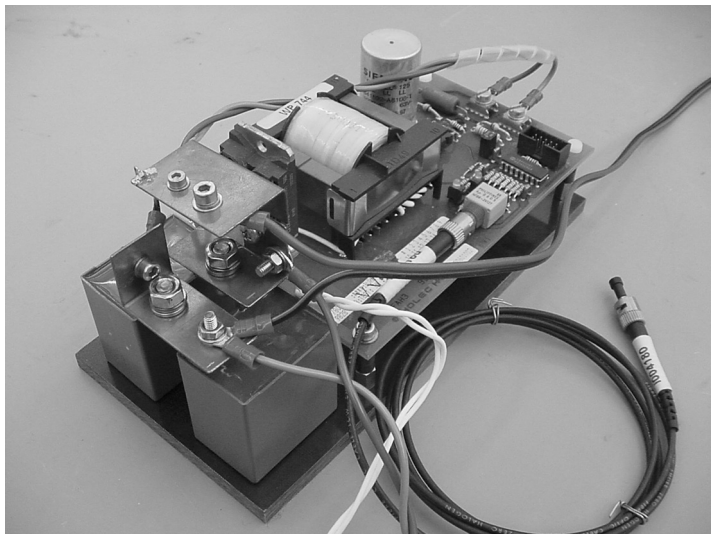

Figure 6. Damped oscillatory circuit and thyristor control electronics.

oscillatory pulses in the μs-range. This damped oscillatory RLC circuit, including the control electronics, is shown in Figures 6 and 7(b). The pulsed measurements were compared with DC experiments (Figure 7(a)), which were carried out with commercially available instruments.

DC Measurements

Both clamped and wetted samples were fed with a DC voltage (0–30 V) from an Agilent N5745A power supply as shown in Figure 7(a). The current through and the voltage across the samples were measured shortly (i.e., ~1 s) after turnon with Fluke 189 digital multimeters. For all measurements the voltage was increased to increase the current density. The separate voltage and current readings were used to determine

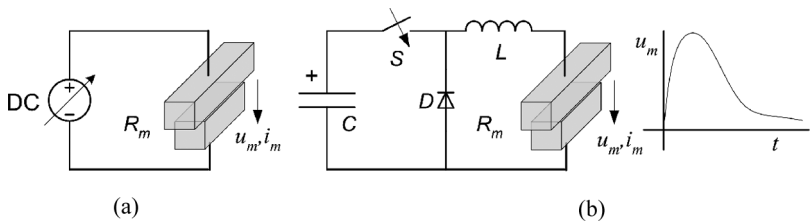

Figure 7. (a) DC measurement setup, (b) RLC circuit used for pulsed measurements with typical waveform.

the measured resistance, R_m, which is used in Equation (3) to calculate the contact resistivity.

Pulsed Measurements

During the measurements, the film acts as a resistive load in an RLC series circuit. The capacitor, which was pre-charged prior to the pulse, energizes the circuit. In general, the circuit generates a waveform with an oscillatory or an exponential decay, which depends on the circuit parameters. [29] To avoid a waveform with zero crossings in the waveform the circuit, which is shown in Figure 7(b), is equipped with an anti-parallel diode, D. The typical values for the parasitical inductor and the capacitor are $\sim 0.5\,\mu H$ and $1.1\,\mu F$ respectively. The resistance, $R = R_m$, which is the sum of the film resistance and the contact resistance, varies per measurement and is typically between 0.1 and$10\,\Omega$. This results in typical pulse length (at 80% amplitude) of approximately $3\,\mu s$.

The capacitor was charged with a current limited power supply (Wallis 10kV/3mA) up to 1.6 kV, which equals a maximum energy of 1.4 J. Release of this energy is done by closing switch S (i.e., firing a thyristor, IXYS MCO 50-16IO1). The diode (BY359) provides the current freewheel path in the case of a capacitor voltage reversal. The thyristor is controlled with a pulse generator (Philips PM5715) and is fired via an optical link and high-frequency driver circuit to ensure galvanic isolation. The experimental setup was equipped with a pre-charged capacitor to limit the amount of dissipated energy during a breakdown and thereby avoid damage to the electrode surfaces. The voltage across and the current through the film sample were measured and used to determine the resistance, R_m, which is used in Equation (3) to determine the resistivity. These measurements were performed with a Yokogawa oscilloscope (DL-1640) and stored afterwards for further processing. For the voltage measurement, a (10:1) probe was been used and current measurements were performed with a Rogowski coil (CWT15A) or Pearson coil (110 A).

Performed Measurements

First, it is necessary to investigate the glue and film conductivity separately. This is described in part I of this contribution. Second, the described clamp is used to determine the electrical characteristics of film and contact resistance together, first without any additional material to improve the connection between film and copper electrodes. In a second experiment, the contact resistance between metal and film was reduced by using a conductive aqueous solution to wet the electrodes. With these

newly obtained values and the conductivity values from glue and film (described in part I) one is able to distinguish the following contact joints:

- Copper-film-copper (r_{s_cf})
- Copper-liquid-film-liquid-copper (r_{s_clf})

The measured resistance, R_m, is a series connection of two or more resistances: the film resistance, which is temperature, pressure, and electric field dependent, and the contact resistance, which is mainly pressure dependent. The total contact resistivity, r_{s_tot}, for each setup is calculated with Equation (3), where n, which is the number of different materials involved in the conduction path, equals 3 and 5 respectively. Since it is impossible to measure a single transition (i.e., from copper to film only) the calculated contact resistivities r_{s_cf} and r_{s_clf} always consist of two transitions (i.e., from copper to film and from film to copper again). So the calculated resistance, r_{s_tot}, needs to be divided by 2 to determine the contact resistivity of one single transition. All measurements described were carried out with the DC setup as well as with the pulsed setup. To determine the exploration range for this material as conductive polymer electrode in pulse power applications, the contact resistivity was determined as function of the current density.

EXPERIMENTAL RESULTS

Contact Resistivity: Film to Bare Copper

With the new detailed conductivity information of the film, one is able to investigate the contact resistivity between film and a bare copper electrode. The determined contact resistivities are:

- $r_{s\_cf} = \mathrm{f(t)}$; $r_{s\_cf} = \mathrm{f(P)}$; $r_{s\_cf} = \mathrm{f(J)}$, with the DC setup
- $r_{s\_cf} = \mathrm{f(J)}$ with the pulsed setup

Due to the visco-elastic properties of the film it will creep under pressure and with time the initial air enclosures between copper and film are filled up which results in a lower contact resistivity. This time- and pressure-dependent resistive behavior was determined at room temperature and is shown in Figures 8(a) and (b) respectively.

Figure 8(a) shows the contact resistivity measured in the clamp with the DC setup ($J < 10^{-5}\,\mathrm{A/mm^2}$) for 3 kPa and 22 kPa applied at $t = 0$. The total resistivity is determined via Equation (3) and divided by 2 to determine the resistivity per transition. These measurements were repeated several times with different electrodes and different film samples. The solid lines show the average values and the dots represent

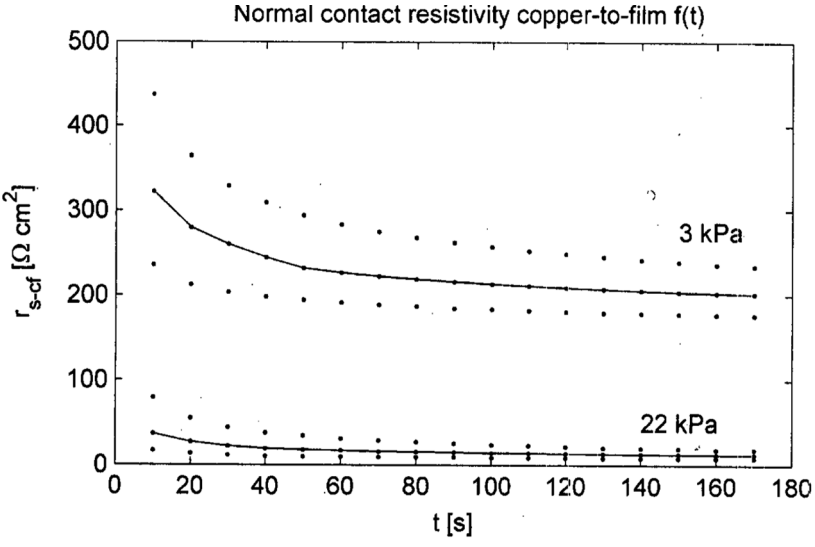

(a)

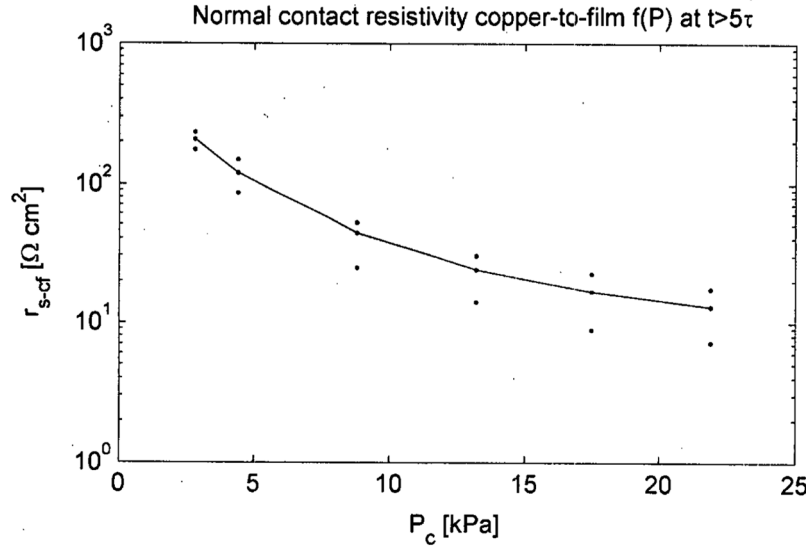

(b)

Figure 8. (a) Contact resistivity in normal direction between copper and film as function of time at an applied pressure of 3 kPa and 22 kPa at $t = 0$, (b) contact resistivity in normal direction between copper and film as function of applied pressure at $t > 5\tau$ (i.e., after the relaxation time of the film).

the minimum and maximum values found. For six different clamp pressures, 2.8 kPa, 4.4 kPa, 8.8 kPa, 13.2 kPa, 17.5 kPa, and 22 kPa the final contact resistivity values were determined and are shown in Figure 8(b). These values were achieved when the readout was stable, after the relaxation time of the film, at least 5τ s. As assumed, higher contact pressures lead to lower contact resistivities. Via the time dependency, shown in Figure 8(a), one is able to estimate the time constant τ defined in part I, which is approximately 20 s and 15 s for 3 kPa and 22 kPa respectively. A closer look at the measured data shows, besides the mentioned fast exponential decay, also a slow decay, with a time constant of approximately 1200 s and 400 s for 3 kPa and 22 kPa pressure respectively. It is generally known that for larger deformations more time constants in the model are needed to obtain accurate results.

Figure 9(a) shows the contact resistance between film and bare electrodes (r_{s_cf}/marked with "o") as a function of the current density

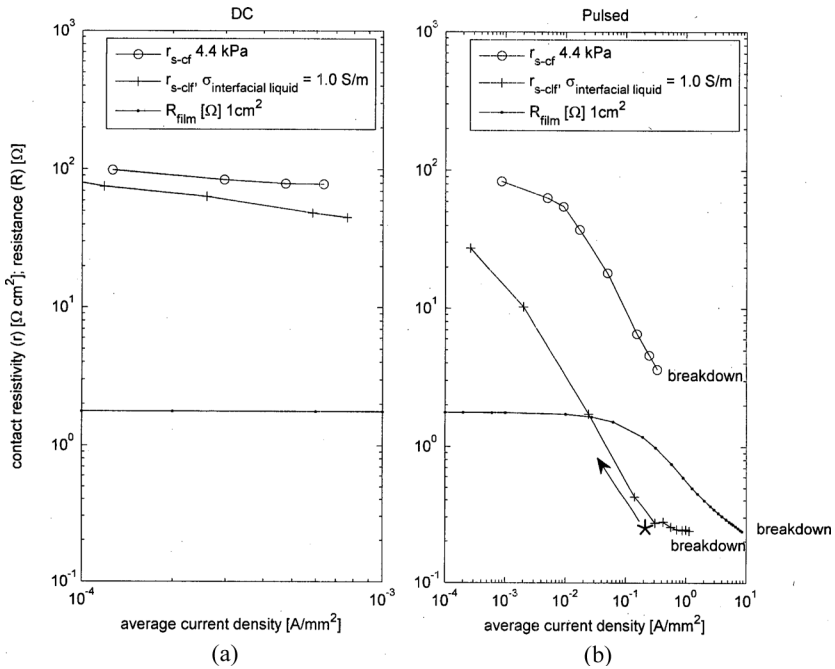

Figure 9. (a) Contact resistivity as a function of the current density for DC operation (left from the dashed line), (b) contact resistivity as a function of the current density for pulsed operation at $\sim$3 µs. Depicted contact resistivities r_{s_cf} and r_{s_clf} are from copper-to-film and copper-to-liquid-to-film respectively. The black dotted line represents the film resistance of $A = 1\,\text{cm}^2$ in normal direction determined in part I, i.e., $R_{film} = \rho(J) \cdot \text{d/A}$, where $\rho(J) = \sigma(J)^{-1}$ and $d = 80\,\mu\text{m}$.

at a pressure of 4.4 kPa measured with the DC setup. The increase in current density has been realized by increasing the voltage in steps. For higher current densities the contact resistivity initially decreases, which will be discussed later. The typical measurement interval between each data point is at least 60 s. The voltage has been applied short (i.e., $\sim$1 s) to avoid excessive chemical reactions and damage to the electrodes, because irreversible electrode (*Red-ox*) reactions will change the chemical nature and the conductivity of the interfacial liquid.

Figure 9(b) shows the contact resistivity between the film and bare electrodes (r_{s_cf}/marked with a "o") as a function of the current density measured with the pulsed setup. Calculation has been done via Equation (3), and the film conductivity is now a function of the current density, $\sigma_f = f(J)$. For higher current densities, a lower contact resistivity can be obtained and for current densities larger than $10^{-2}\,\mathrm{A/mm^2}$ the contact resistivity decreases faster. At low current densities the contact resistivity is 25 times higher than for high current densities. Figures 9(a) and (b) also shows the resistance in normal direction of $1\,\mathrm{cm^2}$ film as a function of the current density (R_{film} marked with a "•"), which relates the contact resistivity to film resistance. It can be seen that for pressurized bare copper film contacts, the contact resistance is always dominating.

Contact Resistivity: Wetted Film to Copper

The experiments carried out with the bare electrodes were repeated with wetted electrodes. If the conductive aqueous solution is homogeneously spread and there are no encapsulated air bubbles, pressure has no influence on the contact resistivity. Figure 9 shows also the contact resistivity from copper-to-liquid-to-film (r_{s_clf}) measured with the DC and pulsed setup both as function of the current density.

Generally due to better utilization of the contact area, the wetted interface has a lower contact resistivity than the pressurized interface. Each data point has been measured shortly ($\sim$1 s) after applying the DC voltage. For both interfaces at DC, bare as wetted as well, the contact resistance dominates above the film resistance.

The contact resistivity of the wetted interface was also measured with the pulsed setup. It behaves the same as the bare interface and decreases with increasing current density, but is much lower in absolute value. For increasing current densities from $1\,\mathrm{mA/mm^2}$ up to $1\,\mathrm{A/mm^2}$, the contact resistivity decreases drastically, from 10 to $0.3\,\Omega\cdot\mathrm{cm^2}$. One is also able to increase the current density further than with bare contacts before breakdown of the sample occurs. This is caused by a better contact between electrode and film and thereby a more homogeneous current

distribution (i.e., more parallel current pathways, as depicted in Figure 3, and less local losses). From $0.3\,A/mm^2$ the contact resistivity becomes more or less constant. The position where the phenomenon happens is marked with an asterisk (*) and depends on the conductivity of the interfacial liquid; it will shift upwards for lower conductivities. For current densities larger then $25\,mA/mm^2$ the contact resistance is no longer dominating above the film resistance.

DISCUSSION

Why does the contact resistivity, depicted in Figure 9, decrease by increasing current density? For the wetted interface as well as for the bare interface this behavior is exhibited. At larger current densities, which can be achieved only in pulsed operation, a much steeper decrease in resistivity was obtained. To be clear, the depicted resistivity decrease is not caused by the increased film conductivity due to the electric field dependence of the film. This behavior has already been compensated, with σ_{film} used in Equation (3) to calculate r_s as a function of the current density J. Two other plausible causes can be assumed. First, at higher current densities and thereby higher field strengths, breakdown of the nonconductive areas, which are caused by thin metal oxides, can occur. These microscopic breakdowns increase the area for current conduction and thereby reduce the contact resistivity. A second possible cause can be the larger influence of migration of ions in the wetted conductive layer, which is the displacement of ions in an electrolyte under influence of an electric field. A larger electric field increases the average ion speed towards the electrodes (i.e., $\nu = \mu E$, where μ is the ion mobility in $[m^2/V \cdot s]$ and E the electric field in [V/m]). Typical values for ν at $2\,kV/mm$ are $0.1\,\mu m/\mu s$. So at higher electric fields the ion concentration, and thereby charge concentration, ρ, near the electrode will be higher, which results in a lower local resistance (i.e., higher local conductivity) of the electrolyte. The conductivity is stabilized when all available ions are separated; this point is marked with an asterisk (*) in Figure 9. In general, the conductivity of the interfacial electrolyte equals $\sigma_e = \rho^+\mu^+ + \rho^-\mu^-$, where ρ $[C/m^3]$ and μ $[m^2/V \cdot s]$ are the charge density of the ions and the ion mobility of the positive and negative ions, respectively.

CONCLUSIONS

A new method has been proposed that enables conductive foils to be characterized with respect to pulsed power applications. Three different methods to reduce the contact resistivity have been compared: pressing, wetting, and gluing. By applying a pressure between 3 and 22 kPa the

typical DC contact resistivities between the investigated polymer film (Carbostat) and bare copper electrodes are generally 200–10 $\Omega \cdot cm^2$. In this pressure range there is no influence on the film conductivity itself, so the decrease in resistance has been reached only by better utilization of the contact area. For higher current densities the contact resistivity decreased further and reached 3 $\Omega \cdot cm^2$ at 0.3 A/mm^2. In the wetted situation the same behavior has been obtained; higher current densities result in lower contact resistivities, typically from 200 to 0.3 $\Omega \cdot cm^2$. At the same current density (i.e., 0.3 A/mm^2), the wetted contact resistivity is 10 times lower than the bare contact resistivity. In the wetted situation the contact resistance is independent of the applied pressure, because all air-encapsulated areas are filled with the conductive aqueous liquid and already contribute to the current conduction.

In general, the glued connection, which is used to determine the film properties (part I), is far superior, but for non-fixed connections the wetted solution is prevalent. Breakdown for the glued, wetted, and bare interface between copper and film occurs at a current density of 8.5 A/mm^2, 1.1 A/mm^2, and 0.3 A/mm^2 respectively.

REFERENCES

[1] Foulger, S. H. (1999). Reduced percolation thresholds of immiscible conductive blends of poly(ethylene-co-vinyl acetate) and high density polyethylene. *J. Polym. Sci. B Polym.* **37**, 1899–1910.

[2] Bloor, D., K. Donnelly, P. J. Hands, P. Laughlin, and D. Lussey. (2005). A metal–polymer composite with unusual properties. *J. Phys. D: Appl. Phys.* **38**, 2851–2860.

[3] Chen, G. H., W. G. Weng, D. J. Wu, and C. L. Wu. (2003). *Eur. Polym. J.* **39**, 2329–2335.

[4] Balberg, I. (2002). A comprehensive picture of the electrical phenomena in carbon black-polymer composites. *Carbon* **40**, 139–143.

[5] Huang, J.-C. (2002). Carbon black filled conducting polymers and polymer blends. *Adv. Polym. Technol.* **21**(4), 299–313.

[6] Andrews, R., D. Jacques, M. Minot, and T. Rantell. (2002). Fabrication of carbon multiwall nanotube/polymer composites by shear mixing. *Macromol. Mater. Eng.* **287**, 395–403.

[7] Makadsi, M., Y. Ramadin, M. Ahmad, A. Zihlif, A. Paesano, E. Martuscelli, and G. Ragosta. (1996). Study of Hall effect on laminated carbon fibre-epoxy composite. *J. Mater. Sci. Lett.* **15**, 547–549.

[8] Huang. C.-Y., and C.-C. Wu. (2000). The EMI shielding effectiveness of PC/ABS/nickel-coated-carbon-fibre composites. *Eur. Polym. J.* **36**, 2729–2737.

[9] Brice, C. W. (1996). Review of technologies for current-limiting low-voltage circuit breakers. *IEEE Trans. Ind. Appl.* **32**(5), 1005–1010.

[10] Doljack, F. A. (1981). Polyswitch PTC devices—A new low-resistance conductive polymer-based PTC device for overcurrent protection. *IEEE Trans. Components Technol.* **4**(4), 372–378.

[11] Schoch, K. F. (1992). Assessment of applications of conducting polymers in power equipment. *IEEE Trans. Power Deliv.* **7**(4), 1681–1687.
[12] Rosner, R. B. (2001). Conductive materials for ESD applications, an overview. *IEEE Trans. Device Mater. Reliab.* **1**(1), 9–16.
[13] International Organization for Standardization. (1999). Measurement of resistivity of conductive plastics. NEN-EN-ISO 3915.
[14] International Organization for Standardization. (2000). Methods of test for determining the resistance and resistivity of solid planar materials used to avoid electrostatic charge accumulation. NEN-EN-IEC61340-2-3.
[15] Roodenburg, B., P. G. Malchev, S. W. H. de Haan, T. I. V. Leitão, and J. A. Ferreira. (2008). Conductive carbon loaded polymer film electrodes for pulsed power applications. Part I: Determination of the film properties. *Int. J. Polym. Anal. Charact*. **13**, 395–412.
[16] Stauffer, D., and A. Aharony. (2003). *Introduction to Percolation Theory*. London: Taylor & Francis.
[17] Carbostat, http://www.romex.nl
[18] Slade, P. G. (1999). *Electrical Contacts: Principles and Applications*. New York: Marcel Dekker.
[19] McIntyre, D. A. (1966). A study of evaporated nickel chromium films as potentiometer tracks. *Microelectron. Reliab.* **5**, 7–10.
[20] O'Callaghan, P. W., and S. D. Probert. (1988). Reducing the thermal resistance of a pressed contact. *Appl. Energy* **30**, 53–60.
[21] Berger, H. H. (1972). Contact resistance and contact resistivity. *J. Electrochem. Soc.* **119**, 507–514.
[22] Cao, A., P. Yuen, and L. Lin. (2007). Microrelays with bidirectional electrothermal electromagnetic actuators and liquid metal wetted contacts. *J. Microelectromech. Syst.* **16**(3), 700–708.
[23] Kupke, M., K. Schulte, and R. Schüler. (2001). Non-destructive testing FRP (fibre-reinforced polymers) by d. c. and a. c. electrical methods. *Compos. Sci. Technol.* **61**, 837–847.
[24] Schoch, K. F. (1994). Update on electrically conductive polymers and their applications. *IEEE Elec. Insul. Mag.* **10**(3), 29–32.
[25] Murakami, Y., N. Hozumi, and M. Nagao. (2004). Surface temperature measurement and analysis of thermal breakdown with ethylene-vinyl acetate copolymer in room-temperature region. *Jpn. J. Appl. Phys.* **43**(9 A), 6184–6187.
[26] Kreuger, F. H. (1995). *Industrial High DC Voltage*. Delft: Delft University Press.
[27] Lide, D. R., ed. (2007–2008). *CRC Handbook of Chemistry and Physics*, 88th ed. Boca Raton, Fla.: Taylor and Francis.
[28] Roodenburg, B., J. Morren, H. E. Berg, and S. W. H. De Haan. (2005). Metal release in a stainless steel pulsed electric field (PEF) system; Part I: Effect of different pulse shapes; theory and experimental method. *Innov. Food Sci. Emerg. Technol.* **6**, 327–336.
[29] De Haan, S. W. H., and P. R. Willcock. (2002). Comparison of the energy performance of pulse generation circuits for PEF. *Innov. Food Sci. Emerg. Technol.* **3**, 349–356.